



The influence of hydrothermal aging on E-glass and S-glass fiber/epoxyreinforced composite pipes

Sujith Bobba^{a,*}, Z. Leman^{a,b}, E.S. Zainudin^a and S.M. Sapuan^{a,b}

^aDepartment of Mechanical and Manufacturing Engineering, Faculty of Engineering, Universiti Putra Malaysia, 43400 Serdang, Malaysia.

^bAdvanced Engineering Materials and Composites Research Centre, Faculty of Engineering, Universiti Putra Malaysia, 43400 Serdang, Malaysia.

Received 03 July 2019,
Revised 29 Aug 2019,
Accepted 30 Aug 2019

Keywords

- ✓ E-glass,
- ✓ S-glass,
- ✓ composite elbow pipe joints,
- ✓ monotonic burst pressure,
- ✓ impact performance

sujith.bobba@mail.com,
zleman@upm.edu.my

Abstract

This research examines the consequences of low-velocity impact loadings and distilled water ageing on E-glass and S-glass fiber-epoxy reinforced composite pipes that were exposed to internal burst pressure and followed by axial compression. The composite pipes, which comprised of four defiant symmetric layers with $(\pm 55^\circ)^3$ winding angles, were produced by the filament winding procedure. The samples were reduced from the pipes to the required experimental length. The samples were then immersed in 90 °C water for the time period intermissions of 600, 1200, and 1800h. The impact heaps of three various dissimilar energy intensities (7.5 J, 10J, and 12.5 J) were employed and pursued by monotonic internal burst pressure and axial compression tests. SEM pictures were taken and the relationship between the ageing period and the point of impact of the composite pipes was identified. The results show that the internal burst pressure failures are contingent to the applied impact energies. Finally, it can be concluded that the burst pressure and the compression behaviours of the conditioned specimens are significantly reduced due to environmental ageing.

1. Introduction

In today's oil and gas industry, glass fiber reinforced epoxy composite pipes have been used considerably for the transportation of extremely harsh fluids. The glass fiber reinforced epoxy composite pipes can remain intact for several years before showing traces of dreadful conditions on the composite's mechanical properties. Fibres and matrix structure can be affected by moisture [1], UV radiation [2], salts [3–5], alkalis and acids [6]. Hu and Sun [7] found that the durability of polymeric composites are affected by moisture and oxidation; in which the moisture percentage release rate depends on the elastic observances. The influence of the composite mechanical properties by fluids is in a way that it can cause degradation of the properties of the composite materials which produces time reliant material reactions. This occurs when the matrix fluctuates and causes degradation of the glass fiber/matrix bond [8, 9]. M. S. Abdul Majid et al. [10] discovered that the behavior of glass fiber reinforced epoxy pipes is influenced by hydrostatic and biaxial load circumstances at improved temperatures. It was observed that the failure of the glass fiber reinforced epoxy pipes is highly reliant on the analysis temperatures. Felipe et.al. [11] investigated glass fiber reinforced plastic sheets by examining the external layers for ecological wear, when they were positioned in a constructed chamber as well as their mechanical behaviour when exposed to uniaxial tension. Rao et al.[12] examined the extent of degradation of glass fiber reinforced plastics laminates under various

environmental impacts. The results showed that the flexural modulus and tensile strength were reduced gradually in the case of GFRP samples when exposed to water immersion at different temperatures. Ramya Krishna et al. [13] performed several tests on cured glass/epoxy composite samples that were exposed to distinctive schedules at 50, 60, 70, and 85°C intervals when immersed in distilled water at 50°C. The consequences of different after-treatment programs, with the moisture diffusion features of the composite were reviewed. Gning et al. [14] confirmed that the damage origination in glass fiber reinforced epoxy pipes showed to impact tests followed by quasi-static below water actions. Based on the outcomes, it was determined that the impact damage can reduce the residual implosion strength of glass fiber reinforced epoxy pipes. By using the similar process as stated above, Kara et al. [15] utilized low velocity impact and monotonic internal pressure tests on filament wound glass fiber reinforced epoxy pipes. Conversely, the researchers operated the tubes with 32 bars internal burst pressure throughout the low velocity impact tests. They observed that for every impact energy applied the damage region for the non-initial stressed tubes were greater than the initial stressed tubes. Chang [16] studied on the failure method of undamaged and damaged graphite epoxy cylindrical tubes that were exposed to three different internal pressures. The deprivation of the relative burst pressure was discovered to be related with the existing local damage of the samples. The major purpose of this study is to examine the consequences of hydrothermal aging under unusual environmental conditions on operation and strength of E-glass and S-glass fiber/epoxy reinforced pipes.

2. Experimental details

2.1 Material and sample preparation

Glass epoxy pipes were manufactured using a controlled filament winding machine with $(\pm 55^\circ)^3$ winding angle. E-glass and S-glass fibres with a density of 1140 tex and a diameter of 18 μm were employed as the reinforcing fabric. An inner radius of 100mm, an outer radius of 101.75mm were used as the dimensions for the fabrication of E-glass and S-glass fiber/epoxy reinforced pipes. Polyester resin ETERSET (2960P-5) and hardener were selected as the matrix for E-glass elbow joint, and in the case of S-Glass elbow joint N-Matrix type resin N,N diglycidyl-4-glycidyoxyaniline ($\text{C}_{15}\text{H}_{19}\text{NO}_4$) supplied by Sigma-Aldrich [17] was cross-linked with meta phenylene diamine ($\text{C}_6\text{H}_8\text{N}_2$) supplied by Zhejiang Amino-Chem Co., Ltd., which is typically used for marine applications [18] as shown in Figure 1 below. The E-Glass and S-Glass elbow pipe joints used for tests and their mechanical properties are presented in Figure 2 and Table-1 below.

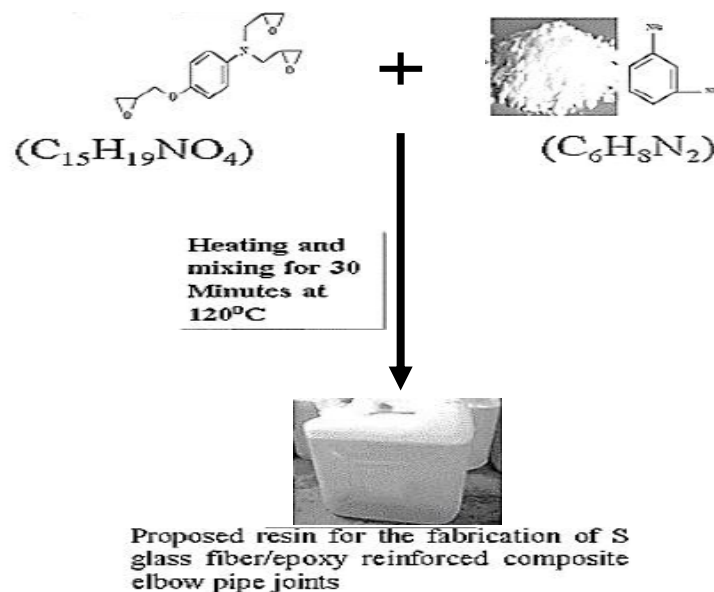


Figure 1: Preparation of proposed resin for the fabrication of the S- glass fiber/epoxy composite pipes as per ASTM STP 569 Standards [16]

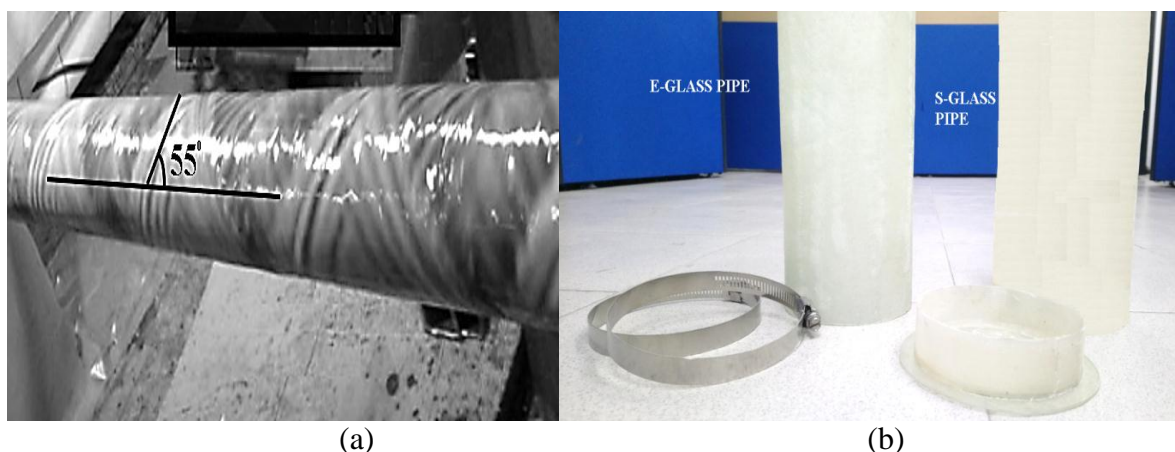


Figure 2: (a) Filament winding process of E-glass and S-glass fiber/epoxy composite pipes. The inset represents winding angle as $\pm 55^\circ$, (b) E-Glass and S-Glass fiber/epoxy composite pipes used for tests

Table-1: The mechanical properties of the E glass fibre, the S glass fibre and the resin

Data provided by the manufacturer	E-glass	S-glass
Thickness of the glass fiber in GSM	900	630
Tensile strength, n/mm ²	2000 Mpa	4750 Mpa
Density, g/cm ³	2.55 g/cm ³	2.43 g/cm ³
Ultimate strain, %	4.5	3.2

3. Experimental Procedure

3.1 Hydrothermal ageing process

The venerable conditions of the E-glass and S-glass fiber reinforced epoxy composite pipes were attained by submerging the pipe samples in normal distilled water for 600, 1200, and 1800 hours in an isolated tank with the dimensions of 44 inches in length, 27 inches in breadth, 31 inches in height and the wall thickness of 2.5mm, as shown in Figure 3. The hydro thermal ageing process was performed until the water reached the utmost diffusion state. Water temperature was sustained at 90 °C to speed up the ageing activity. Temperature in the container was regulated by using a copper immersion heater with the capacity of 4 kW and attached by PIC microcontroller to monitor the temperature. The percentage of absorption of water by the samples was governed in accordance to the ASTM D570 standard [19]. Water engagement was analysed by the weight gained by the immersed samples to the weight of the dry samples. Three glass fiber reinforced epoxy pipes fabricated with E-glass and S-glass fibres were tested. The tank was closed using a lid and fastened on all sides to prevent dispersion of heat.

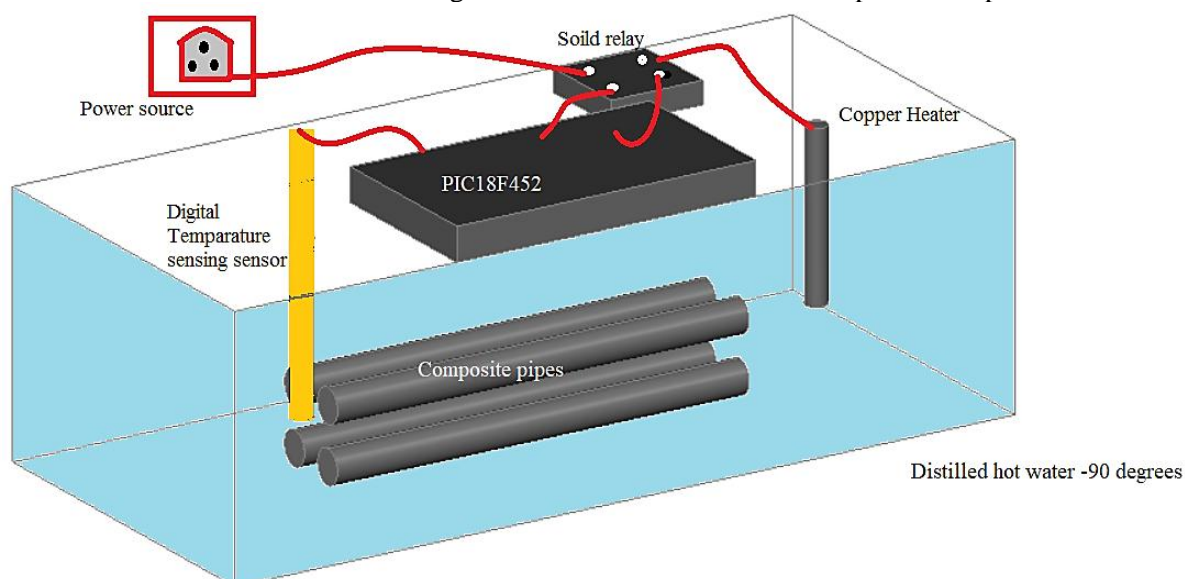


Figure 3: Diagrammatic representation of composite pipes under hydrothermal ageing process

3.2 Impact tests

Typically, impact resistance alongside with impact strength is the most commonly considered property to be calculated to predict the damage in the composites. Impact damage can be prophesied by two methods such as impact damage resistance and damage forbearance. In the present, design impact tests were carried out by utilising a machine corresponding to ASTM D2444 standards [20]. The impact machine can be operated for various functions from high to low impact momentums. The impactor holds a hemispherical nose like structure with 12.5mm diameter, which is installed with a 22.3kN piezoelectric force transducer. The overall falling mass with the crosshead, impactor nose and force transducer was 5.04 kg. While performing the impact tests, a bounding structure was used to control the specimens from various impacts. Experiments were performed with different impact energies of 10J, 15J, and 20 J; in order to examine the damage development in different fiber/epoxy composite pipes at room temperature. For the impact tests, a unique apparatus was designed and developed. The fiber/epoxy composite pipes were closed with two glass epoxy lids to create a real composite pipes situation as shown in Figure 4 below; it was rested on the hollow and secured to the bottom plate of the equipment with four nuts and bolts. A high speed camera with a hotshot SC software was used to predict the contact time between the specimen and the impactor as shown below in Figure 4.



Figure 4: The setup of IMATEK Ltd drop impact testing machine and the test jig used for impact testing.

3.3 Monotonic Burst Tests

The quick interval burst pressure tests were implemented with a minimum of four samples corresponding to ASTM D1599 standard [21] as shown in Figure 5 and Figure 6. A built free apparatus was utilized for quick interval hydraulic burst pressure. The equipment permits the composite pipe to contract and to increase in the

diameter liberally which enables the calculation of the axial stress of the composite pipe. The inner pressure was produced by a hydraulic pump. Throughout the investigation, pressure inside the pipe was constantly and evenly increased until failure occurred. Internal pressure test intervals were calculated until the composite sample collapsed to a specific load rate.

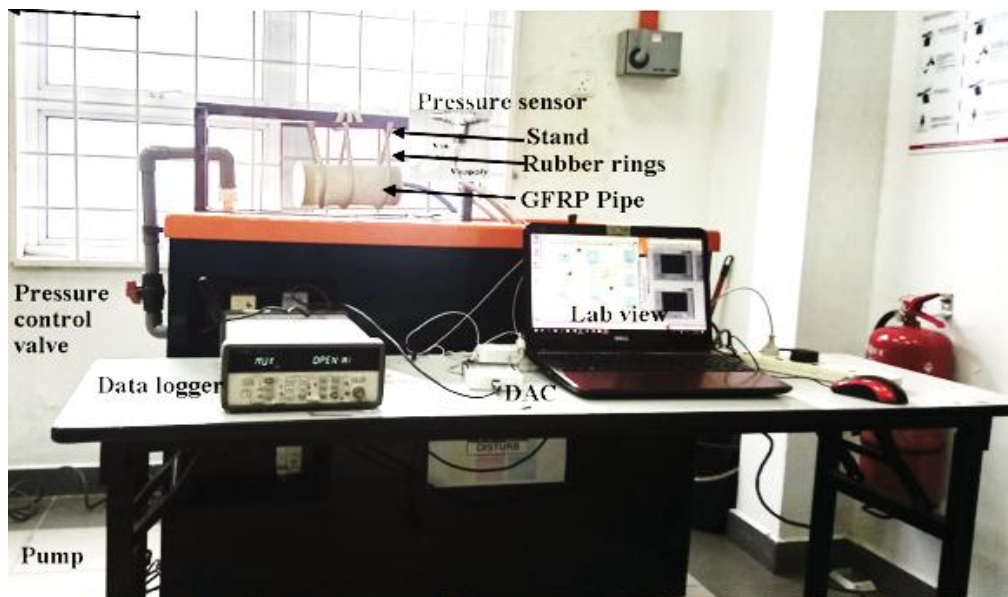


Figure 5: Monotonic burst pressure test rig designed according to ASTM D1599[22]

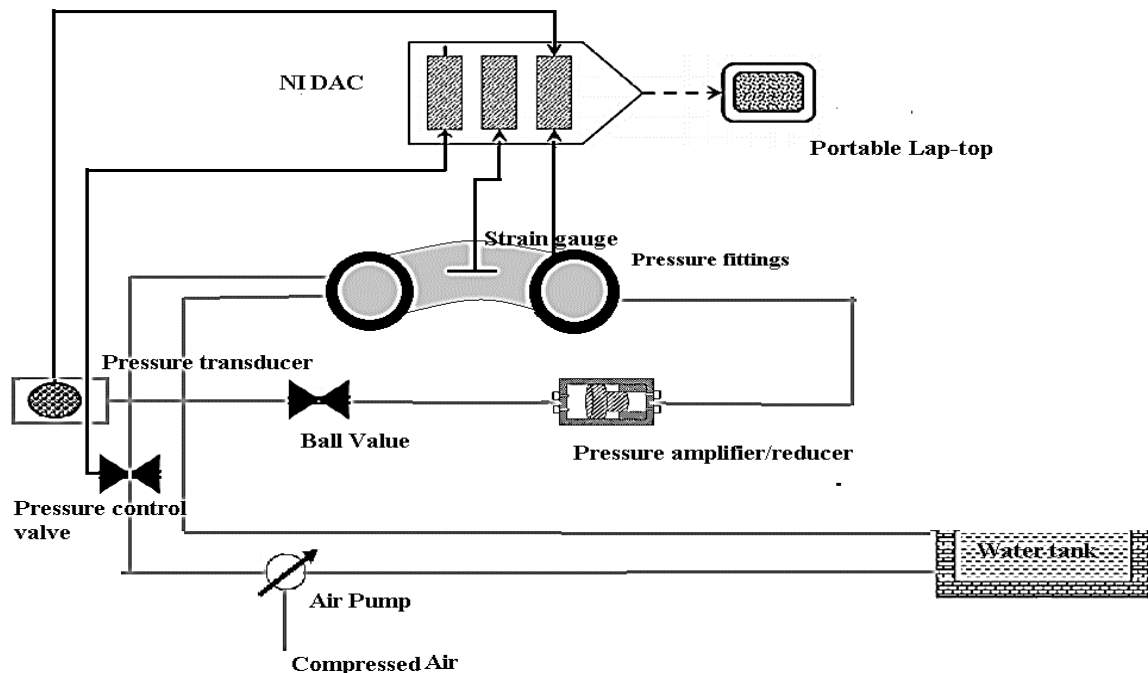


Figure 6: Diagrammatic representation of the automated pressure test rig

3.4 Axial Compression Tests

Compression tests after impact and internal pressure tests were conducted by employing an INSTRON-1195, which has a capacity of 500 KN as per ASTM D695 – 15 Standard [22] as shown in Figure6. The samples were subjected to loading at a constant cross-head speed of 2.5 mm/min. The elbow pipe joint was compressed axially using two plates with a fixed size. Based on the present work, the Glass Fiber/epoxy Composite elbow joints were subjected to axial compression tests until failure occurred at the contact point between the both ends of the pipe and the compression plates of the test machine.

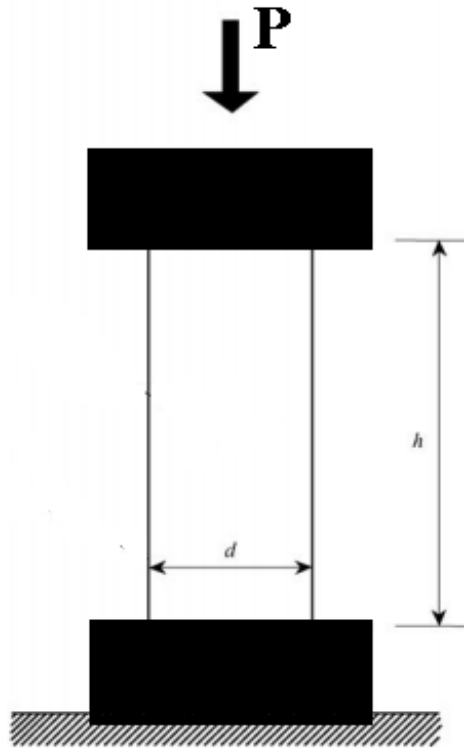


Figure 7: Axial compression test machine with closely fitted pipe with epoxy lids and the process of applying axial load

The main problem during the compression test is the failure formed at the end of the pipe that was the contact point between the tube ends and the plates of the compression test machine. This failure occurred before obtaining the real compression strength of the pipes. To prevent the sample from this premature failure, the tubes were closed with two glass–epoxy lids at both ends, as shown in Figure 7. In the compression tests, a data acquisition system records the axial force –strain history.

4. Results and discussion

4.1 Moisture absorption behaviour

Ageing and diffusion is initiated by plasticisation of the immediate neighbouring molecules in the resin matrix, and swelling is caused by moisture absorption. The proportion of dispersion of water from composite pipe depends on various factors such as the type of the resin layer, fiber dimension, fiber alignment, fiber volume fraction, permeability and holes. Moisture consumption, initiated with the swelling of the E-glass and S-glass fiber reinforced epoxy composite pipes, produces an internal stress on the fiber/epoxy interface bonding. Based on prolonged observation, this will lead to the development of cracks in the fiber/epoxy interface. The average rate of moisture absorption during ageing is estimated using the following equation (3).

$$M_c(\%) = \frac{\text{Mass of the moist specimen} - \text{Mass of the dry specimen}}{\text{Mass of the dry specimen}} \times 100\%$$

$$= \frac{M_e - M_d}{M_d} \times 100\% \quad (3)$$

M_t is the water mass gain/change, and M_e and M_d are the mass of the specimen exposed to seawater and dry specimen, respectively.

The fiber/epoxy bonding became flexible with the increase in the hydro water immersion time owing to the higher amount of water absorbed by the composite pipes. This phenomenon caused the E-Glass and S-Glass fiber laminates to soften and the fiber–polyester resin bond to further degrade; since the matrix became pliable owing

to the occurrence of plasticisation [1, 23]. The impact and strength performance of these pipes can be effected by this condition of ageing. As the immersion period increased, the quantity of water molecules existing increased with the decrease in the polyester resin contents and finally resulting in higher possibility of interlaminar shear strength reduction. The stress transmission ability of the composite pipe, however, stays more at lower immersion time due to fiber/resin bond. Comparison of moisture content and hydrothermal ageing time period in hours of E-glass and S-glass fiber/epoxy reinforced composite pipes is shown above in Figure 8.

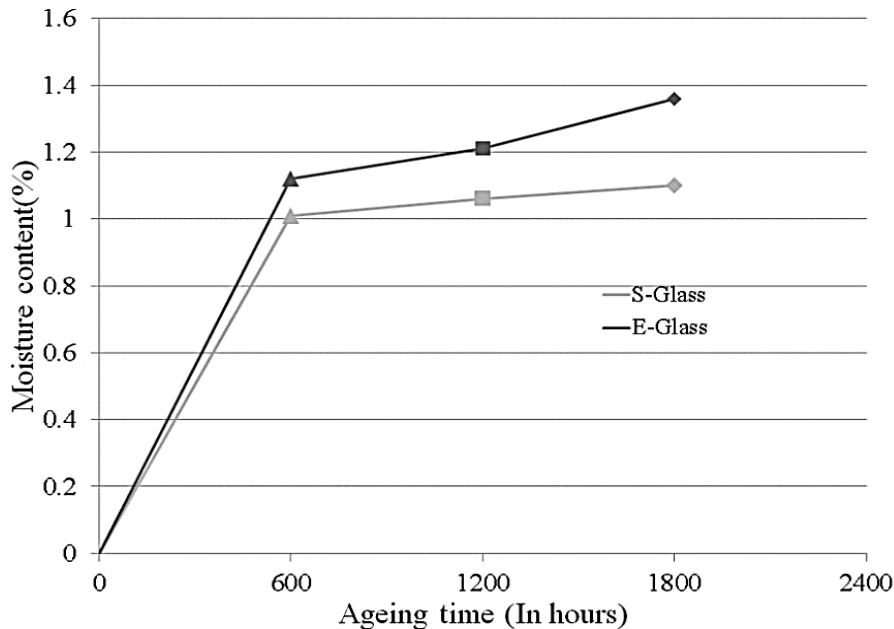


Figure 8: Comparison of moisture content versus hydrothermal ageing time in hours of E-glass and S-glass fiber/epoxy reinforced composite pipes.

4.2 The level of impact loading

A major influence in the fiber/matrix interface can be produced by both hydrothermal ageing and impact response in the E-glass and S-glass fiber/epoxy composite pipes. The force and displacement graphs generated while performing impact tests were noted and analysed. Throughout the process, the damages caused by the impact at various phases were noted. The main slope shaped in the curves designates the elastic phase, in which the composite pipes have undergone initial deformation. The midway slope indicates the plastic phase, caused by initial permanent damage in the form of matrix cracking and delamination, and the final slope denotes the bounce back phenomenon of the striker on the composite pipes which were impacted.

Based on thorough examination, two damages were noticed on the E-glass and S-glass glass fiber/epoxy composite pipes. Fiber/epoxy interface cracking and delamination occurred more on the pipes impacted with 10J and 12.5, but when it came to the point of 7.5 impact damage, only fiber/epoxy inference cracking can be noticed. For the types of material, E-glass composite pipes suffered both matrix cracking and delamination when subjected to 7.5j impact, but in the case of S-glass composite pipe, the damages were observed eventually). The filament wounded S-glass composite pipes showed higher elongation and stiffness to withstand maximum load in all cases, when compared to E-glass composite pipes. Glass fiber rupture and perforation of the impactor were noticed during the tests in the case of E-glass fiber composite pipes for the preferred impact energy intensities.

Figure.9 above projects the force and ageing time graphs of two different materials with three different impact energy levels under un-aged condition. One additional point that can be noticed from the graphs is that for each single level of impact energy, the force decreases with the decrease of aging/immersion time period. The maximum force is more prominent in the case of composite pipe fabricated with E-glass rather than S-glass, and this is similar in the case of aged and un-aged. The ultimate force is extreme in the case of un-matured samples and it reduces progressively with an upsurge in the immersion time period from 600 h to 1800 h. Ultimate forces are recorded for the 1200-h- and 1800-haged samples because of the plasticisation of the matrix

Another significant factor for evaluating the impact characterisation of E-glass and S-glass glass fiber/epoxy composite pipes is the utmost displacement. In an impact test, displacement can be defined as the progress of impact on the pipe exterior surface from the normal state to the impacted state. Figure.10-12 display the displacement to force graph of the impact on tested pipes for all circumstances. Based on the graph, it can be

clearly observed that the displacement surges steadily with the rise in the impact energy for the mature composite pipes. The displacement also amplifies from the E-glass and S-glass glass fiber/epoxy composite pipes which are under dry condition to the 600 hour immersed samples before declining progressively following ageing for 1200 hours. The area below the force and displacement graph denotes that the energy was dispersed due to plastic distortion. The absorbed energy can be calculated mathematically by observing the consequences attained from the force and displacement graphs by means of the subsequent Eq. (4):

$$W = \int F. ds = F_m(S_f - S_i) \quad (4)$$

Energy absorbed by the composite pipe is denoted by W, the mean of the applied force as F_m , the highest displacement as S_f , and finally S_i is the initial displacement for a given impact load.

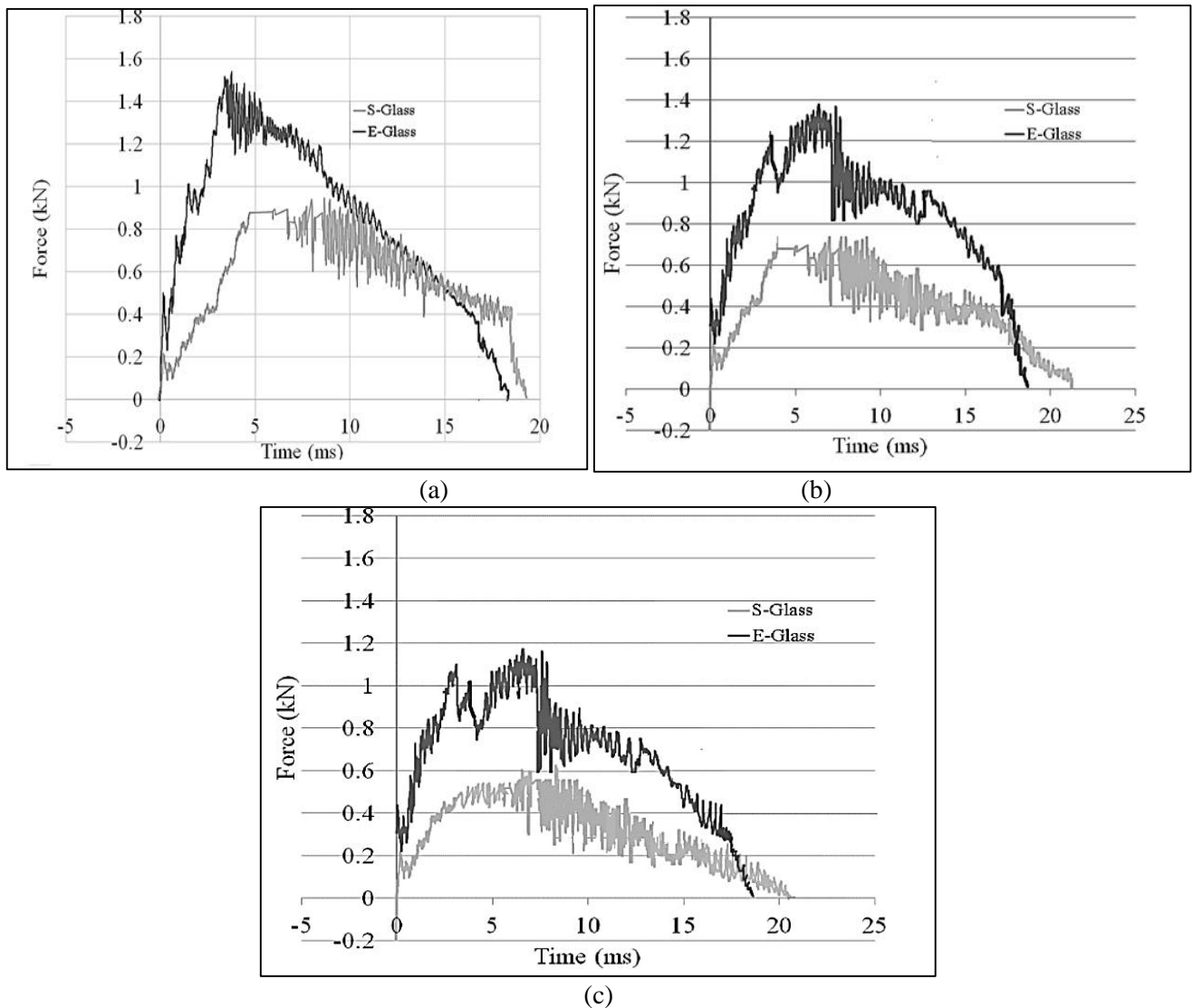


Figure 9: A comparison of force and ageing time of S-glass and E-glass fiber/epoxy reinforced composite pipes at (a) 7.5J, (b) 10J and (c) 12.5J

As can be seen from the above Figures.10-12, the E-glass fiber/epoxy composite pipes at 1800-h- immersion time generally absorbed lesser energy than the S-glass glass fiber/epoxy composite pipes. It can be concluded that the energy absorption on the composite pipe build-ups depends on the energy dispersed by the damaged part. Figure 13 shows an image of the damage that occurred in the vicinity of the impact point of the E-glass and S-glass glass fiber/epoxy composite pipes. The damaged area increased in size with the increase of the impact energy and ageing time.

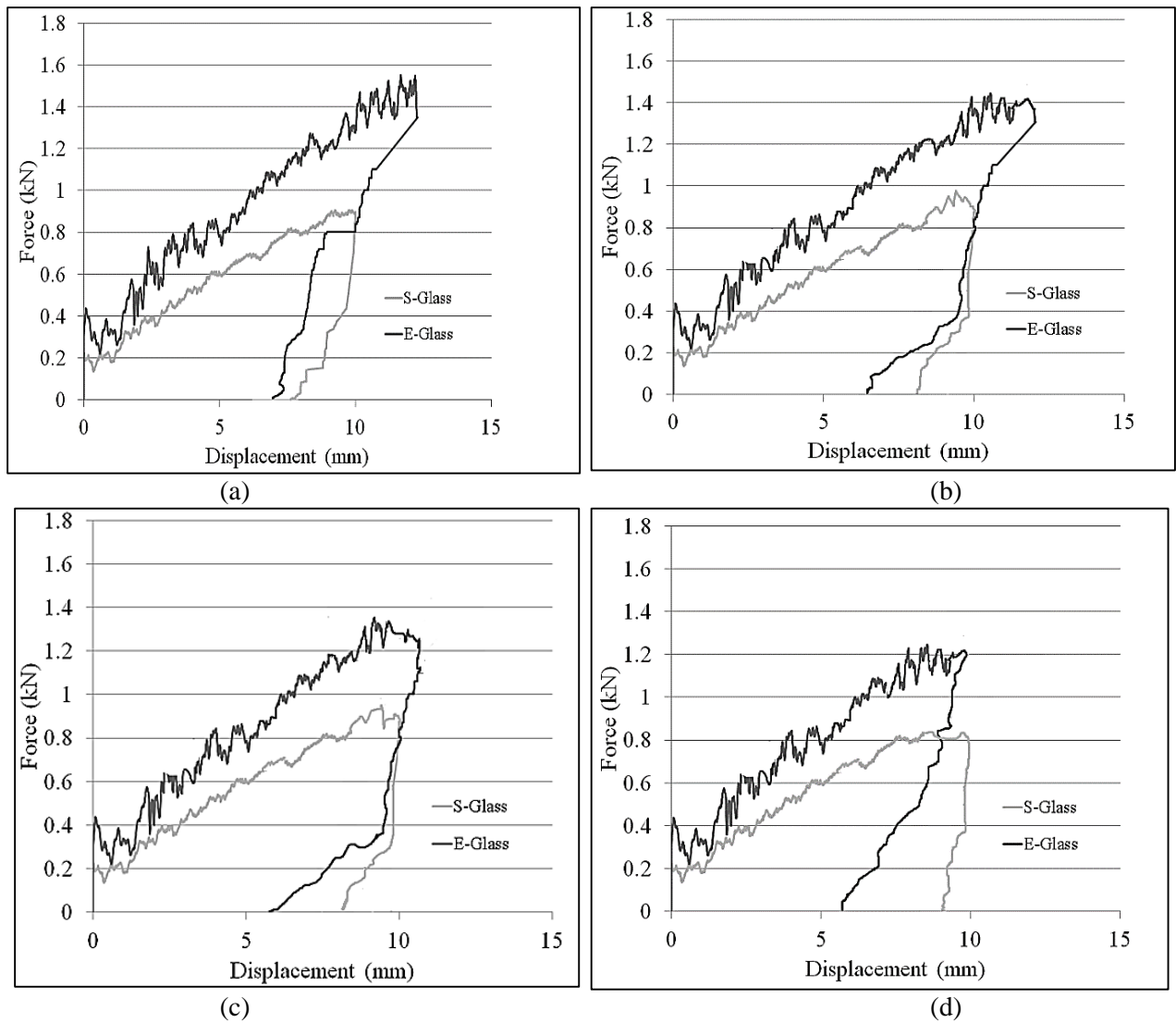
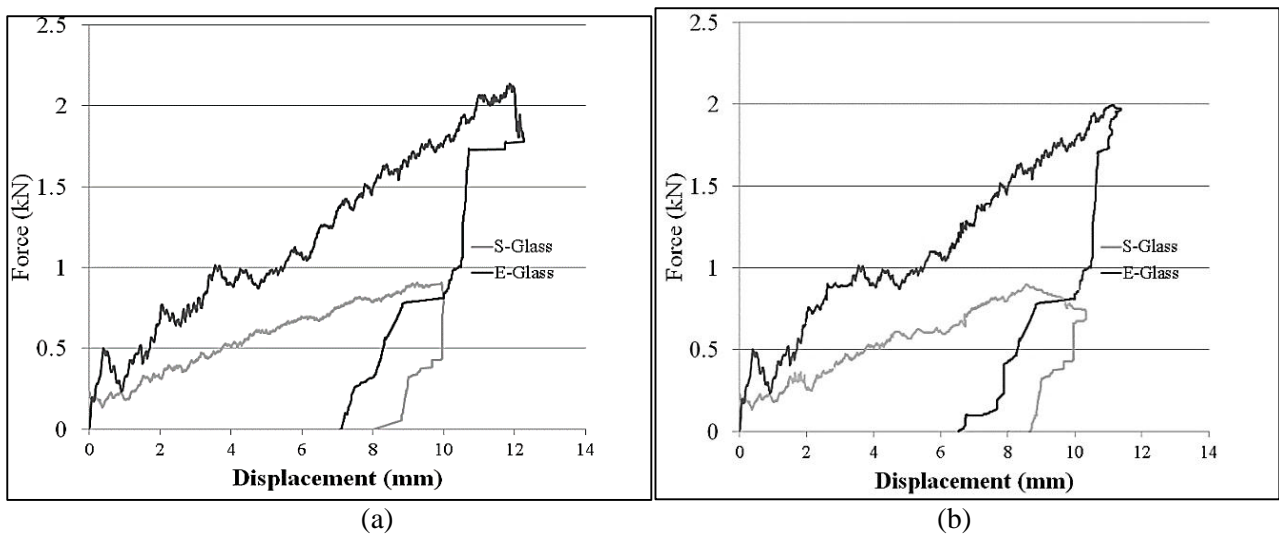


Figure 10: Force–displacement curves with 7.5 J impact energy: (a) dry sample and samples aged for (b) 600 h, (c) 1200 h, and (d) 1800 h



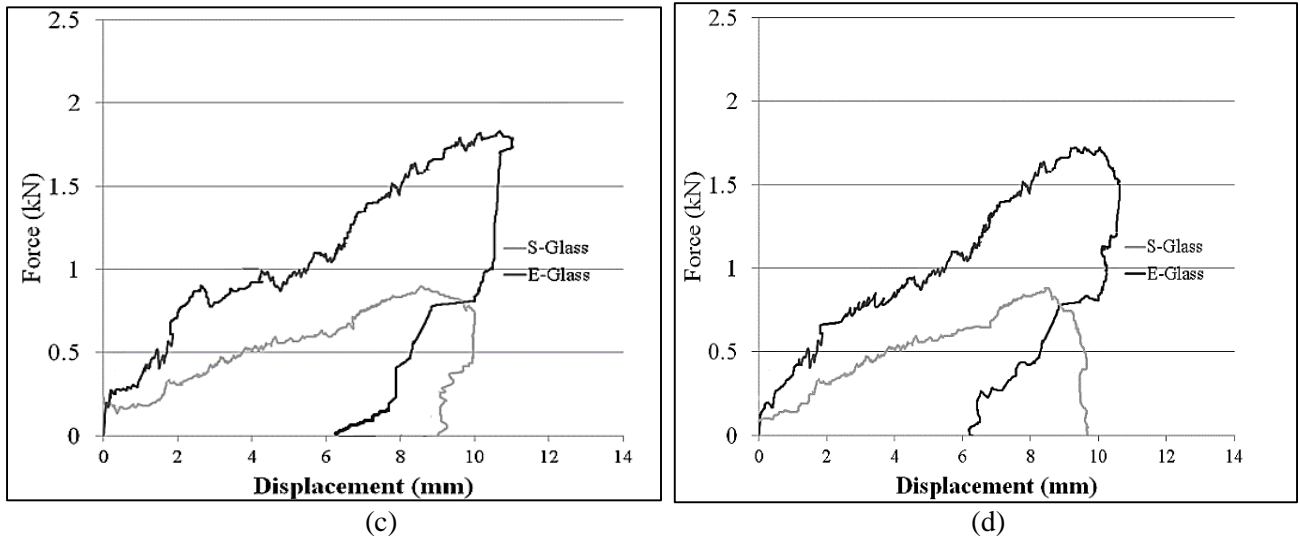


Figure 11: Force–displacement curves with 10 J impact energy: (a) dry sample and samples aged for (b) 600 h, (c) 1200 h, and (d) 1800 h

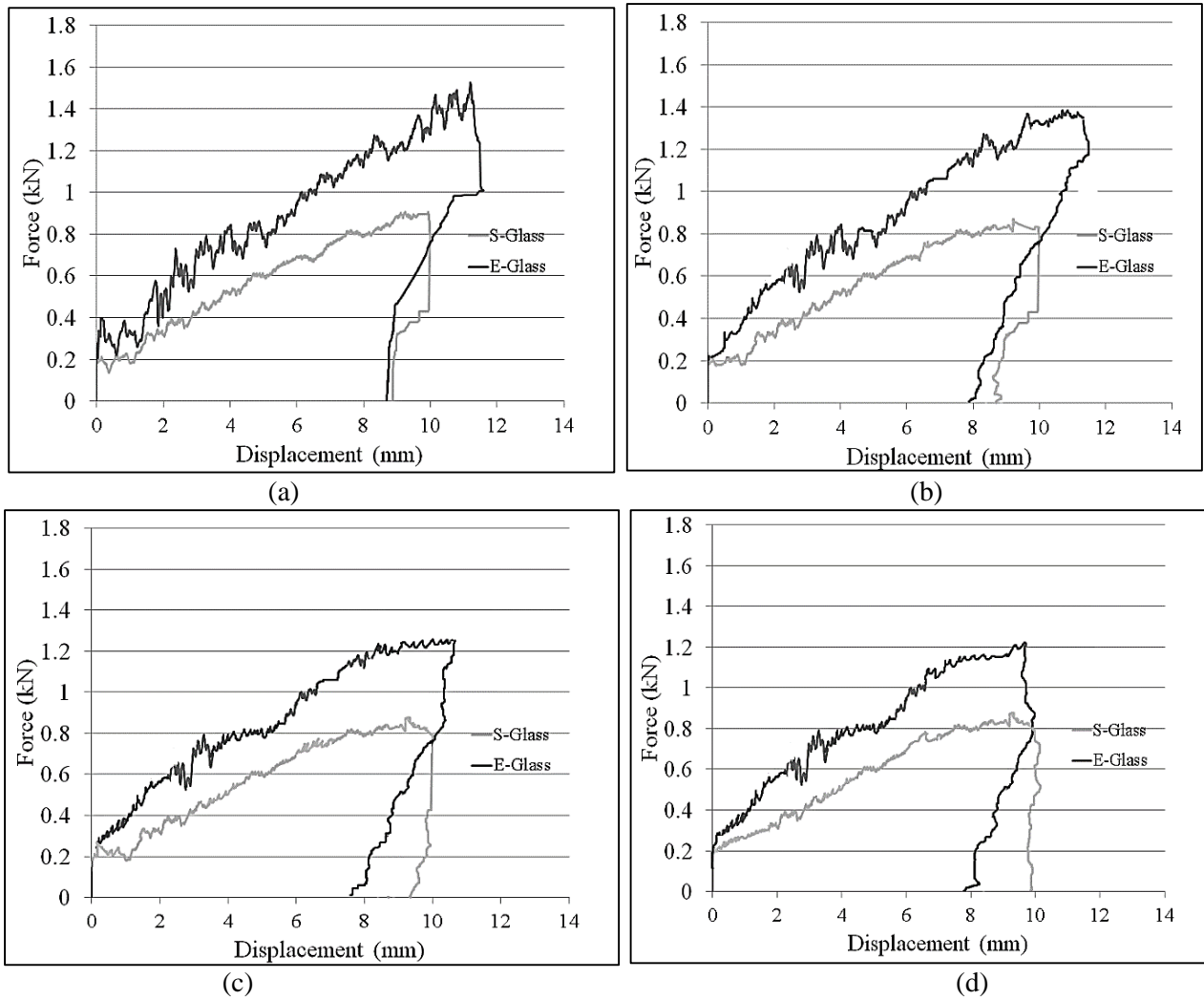


Figure 12: Force–displacement curves with 12.5 J impact energy: (a) dry samples and samples aged for (b) 600 h, (c) 1200 h, and (d) 1800 h

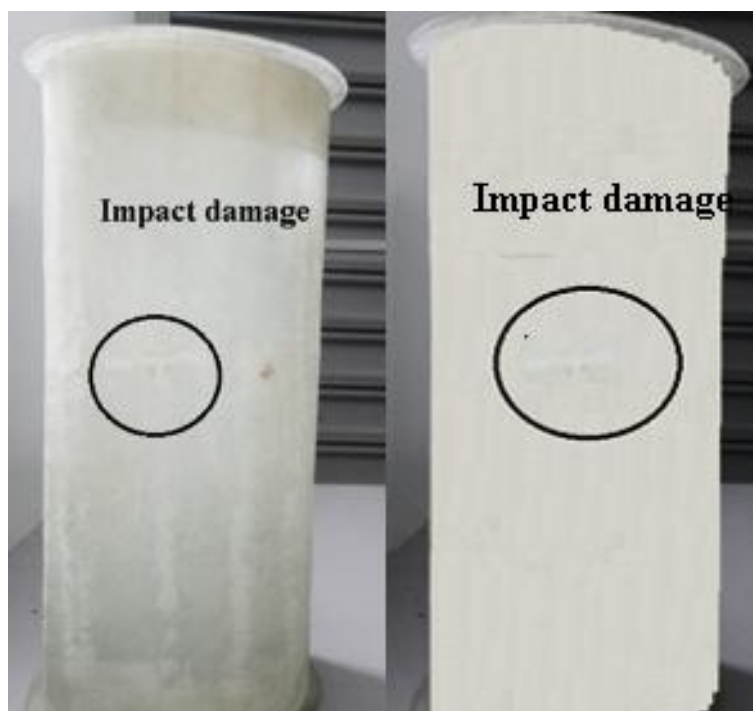


Figure 13: *Damage views of glass fiber /epoxy composite pipe (a) E-Glass (b) S-Glass with a sample impact energy*

4.3 Burst Strength

Monotonic burst tests were performed on the impacted E-glass and S-glass glass fiber/epoxy composite pipes under various pressure sealed conditions. These tests were implemented with the objective of deciding on the composite pipe's internal burst strength once the pipes were exposed to the ageing procedure and the impact loadings of different energies. Composite pipes fabricated with E-glass fiber/epoxy shows higher burst pressure than those fabricated with S-glass fiber/epoxy impacted. Similarly, in the cases of the impact energy levels of 10 J and 12.5 J, lower burst strength is observed as compared to the composite pipes with 7.5J impact energy levels in every distilled water-hydrothermal aged conditions. S-glass fiber/epoxy composite pipes impacted with 7.5J shows burst strength of 70.43MPa, but this value degrades to 43.11MPa and 44.61MPa for the 10-J- and 12.5-J-impacted specimens in distilled water-hydrothermal aged condition for 600 hours. The same phenomenon was observed in the case of hydrothermal aged condition for 1200 hours and 1800 hours. However, in the E-glass fiber/epoxy composite pipes, 7.5J impact composite pipes show a burst strength of 60.04 MPa, where the value degrades to 43.11 MPa. Furthermore, 31.11 MPa is recorded for the 10-J- and 12.5-J-impact composite pipes for the same case above as in S-glass fiber/epoxy composite pipes respectively, implying a strength reduction of more than 30% in both of these cases. Internal burst pressure tests on E- glass and S-glass composite pipe impacted at various energy levels is shown in Table2 below.

As for the aging time, a maximum burst strength is observed for specimen aged 600h when compared to the aging time of 1200 and 1800h. Furthermore, the strain to failure is also generally reduced, with the highest reduction observed at a strain of almost 40% respectively from the 7.5-J- to the 12.5-J-impacted specimens. A deliberate and similar development of water droplets in the region around the impact-damaged area could be detected on the exterior surface of both E-glass and S-glass glass fiber/epoxy composite pipes (Figure 14). As the internal pressure increases, additional droplets were noticed, and once after the substantial build up, the composite pipe surface was enclosed with water, which then trickled from the composite pipe. The outcomes evidently suggest that ageing under water and impact loading have critical results on the burst failure pressure of the E-glass and S-glass fiber/epoxy composite pipes. Therefore, the impact occurrence on under-pressure glass fiber/epoxy composite pipes must be taken into account during their maintenance period.

Table.2: A summary of Internal burst pressure tests on E- glass and S-glass composite pipe impacted at various energy levels

Type	Ageing time (In Hours)	Impact energy(J)	Maximum burst pressure(Mpa)	Axial stress(Mpa)	Hoop stress(Mpa)	Type of failure
E-Glass	600	7.5	5.40	60.04	120.08	weepage-eruption
		10	3.65	43.11	86.23	weepage-eruption
		12.5	2.92	31.11	62.23	eruption
	1200	7.5	4.45	39.77	79.55	weepage-eruption
		10	3.21	32.61	65.23	eruption
		12.5	2.28	27.61	55.53	eruption
	1800	7.5	3.18	32.12	64.25	weepage-eruption
		10	2.23	26.78	53.56	eruption
		12.5	2.01	24.87	49.74	eruption
S-Glass	600	7.5	6.23	70.43	140.87	weepage
		10	5.22	55.12	110.25	weepage-eruption
		12.5	4.98	44.61	89.22	weepage-eruption
	1200	7.5	5.89	56.29	112.58	weepage
		10	4.56	40.62	81.25	weepage-eruption
		12.5	3.22	37.61	75.23	weepage-eruption
	1800	7.5	4.62	49.27	98.54	weepage
		10	3.22	39.25	78.50	weepage-eruption
		12.5	2.99	32.44	64.88	weepage-eruption

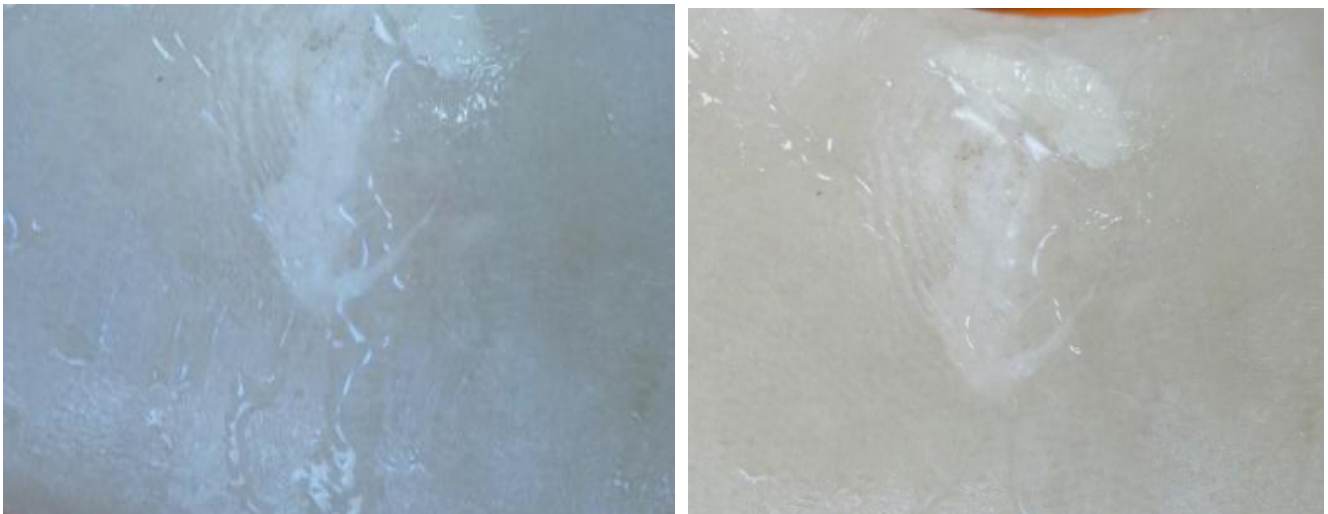


Figure 14: Water leakage at maximum pressure in E-glass fiber/epoxy composite pipes and S-glass fiber/epoxy composite pipes

4.4 Axial compression-after impact and burst pressure tests

Figure 15 shows a photo of the E-glass glass fiber/epoxy composite pipe subjected to compressive loading after impact and burst pressure tests. As can be seen from Figure 15, damages generally occur near the end of the composite pipes due to the local buckling behaviour, especially in the composite pipes fabricated with E-glass fiber. The failure generally propagates from the impact point, except for the specimens made of S-glass fiber. For these pipes, the failure is likely to be resulted from buckling due to the elastic nature of the fiber. The variation of compression-after impact and burst strength of the composite pipes are obtained according to the type of material

and the impact energy levels. Compressive strength does not change significantly for the S- glass specimens; however, in the case of specimens that are fabricated with E-glass, the strength drops suddenly because of buckling.



Figure 15: Compression damage and buckling damage in a sample E-glass fiber/epoxy composite pipe

Finally, [Figure 16](#) shows that there is no serious damage on the E-glass and S-glass glass fiber/epoxy composite pipes. However, on the part of impact damage zone, the main failure mode seems to be of buckling. Also, it is observed that the axial compression-after impact- burst pressure strength increases or decreases with the parameters such as impact energy, internal burst pressure, material and matrix used

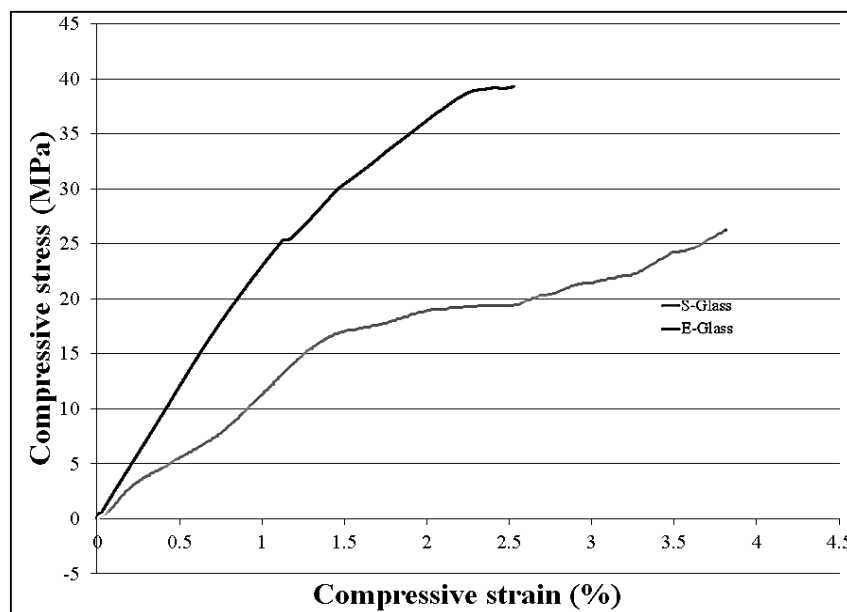


Figure 16: Compressive stress versus compressive strain of E-glass fiber/epoxy composite pipe and S-glass fiber/epoxy composite pipe

Conclusion

The following conclusions are drawn on the basis of results of impact, internal burst pressure and axial compression tests performed on impacted composite pipes under unaged and aged conditions:

1. Glass fiber/epoxy composite pipes made with S-glass fiber, being more variable, consume more energy elastically and the damage is not as much as the pipe joints made of E-glass fiber for a given compression load.
2. The squalor of resin fillings and fibre/matrix connection surges with the increase of ageing period as the additional water molecules existed leach out the resin fillings in the covers, which is followed by the drop in the drop of stress transmission nature in the E-glass and S-glass fiber/epoxy composite pipe
3. From the force versus displacement graphs, it can be noticed that the ultimate force normally rises with the increase of impact energy at individual ageing time period.
4. The highest displacement, the area of the damage and the energy absorbed on the glass fiber/epoxy composite pipe at each separate ageing state is expected to increase as the impact energy surges up.
5. Three damage stages were noticed from the internal burst pressure tests; initially as the internal pressure increased, whitening patch was followed by the occurrence of weepage and eruption let-down.
6. Axial compression tests on glass fiber/epoxy composite pipes with different material provide an indication that due to the effect of buckling, the axial compression strengths of 2.75m, on both E-glass and S-glass fiber/epoxy Composite pipe, are nearly about 38% less than the crushing strengths.

Finally, based on the conducted experiments, rather than using the existing E-glass fiber, implementing the proposed S-glass fiber and resin can reduce the degradation of mechanical properties in the composite pipes due to hydrothermally aging.

Acknowledgment

The authors would like to thank Universiti Putra Malaysia and the Department of Mechanical and Manufacturing Engineering, UPM for supporting this project under a grant by UPM Scheme, Vot No 9556200

References

1. J.R.M. d'Almeida, R.C. de Almeida, W.R. de Lima, Effect of water absorption of the mechanical behavior of fiberglass pipes used for offshore service waters, *Compos. Struct.* 83 (2008) 221–225, <http://dx.doi.org/10.1016/j.compstruct.2007.04.020>.
2. H. Abdullah, A.S. Al, R.A. Siddiqui, The effects of weathering on mechanical properties of glass fiber reinforced plastics (GRP) *Materials*, 1 (2000) 1–6. <https://doi.org/10.31436/iiumej.v1i2.333>
3. E.P. Gellert, D.M. Turley, Seawater immersion ageing of glass-fibre reinforced polymer laminates for marine applications, *Compos. A: Appl. Sci. Manuf.* 30 (1999) 1259–1265, [10.1016/S1359-835X\(99\)00037-8](https://doi.org/10.1016/S1359-835X(99)00037-8).
4. H. Gu, Behaviours of glass fibre/unsaturated polyester composites under seawater environment, *Mater. Des.* 30 (2009) 1337–1340, <http://dx.doi.org/10.1016/j.matdes.2008.06.020>.
5. M.E. Deniz, R. Karakuzu, Seawater effect on impact behavior of glass–epoxy composite pipes, *Compos. Part B* 43 (2012) 1130–1138, <http://dx.doi.org/10.1016/j.compositesb.2011.11.006>.
6. A.M. Amaro, P.N.B. Reis, M.A. Neto, C. Louro, Effects of alkaline and acid solutions on glass/epoxy composites, *Polym. Degrad. Stab.* 98 (2013) 853–862, [10.1016/j.polymdegradstab.2012.12.029](https://doi.org/10.1016/j.polymdegradstab.2012.12.029)
7. H. Hu, C. T. Sun, “The Characterization of physical aging in polymeric composites”, *Compos. Sci. Technol.* 60 (2000) 2693-2698.
8. J. Yao, G. Ziegmann, “Equivalence of moisture and temperature in accelerated test methods and its application in prediction of long-term properties of glass-fiber reinforced epoxy pipe specimen”, *Polymer Testing*, 25 (2006) 149-157.
9. Julien Mercier, Anthony Bunsell, Philippe Castaing, Jacques Renard, “Characterisation and modelling of ageing of composites”, *Composites: Part A*, 39 (2008) 428-438.

10. M. S. Abdul Majid, T. A. Assaleh, A. G. Gibson, J. M. Hale, A. Fahrer, C. A. P. Rookus, M Hekman, "Ultimate elastic wall stress (UEWS) test of glass fibre reinforced epoxy (GRE) pipe", *Composites: Part A*, 42 (2011) 1500-1508.
11. R. N. B. Felipe, R. C. T. S. Felipe, E. M. F. Aquin, Laminar composite structures: Study of environmental aging effects on structural integrity, *Jourl. of Reinf. Plast. and Comp.* 31 (2012) 1455- 1466
12. P. Sampath Rao, M. M. Husain, D. V. Ravi Shankar, An Investigation on Strength Degradation of GFRP Laminates under Environmental Impact, *Inter. Jour. of Comp. Materls.* 2(4) (2012) 48-50.
13. Ramya Krishna, A. Revathi, S. Srihari, R. M. V. G. K. Rao, (2010). Postcuring Effects on Hygrothermal Behavior of RT-cured Glass/Epoxy Composites, *Jour. of Reinf. Plast. and Comp.* 29 (2010) 325-330, <https://doi.org/10.1177%2F0731684408097767>
14. P.B. Gning, M. Tarfaoui, F. Collombet, P. Davies, Prediction of damage in composite cylinders after impact, *J. Compos. Mater.* 39 (2005) 917–928, <http://dx.doi.org/10.1177/0021998305048733>
15. M. Kara, M. Uyaner, A. Avci, A. Akdemir, Effect of non-penetrating impact damages of pre-stressed GRP tubes at low velocities on the burst strength, *Compos. Part B* 60 (2014) 507–514, [10.1016/j.compositesb.2014.01.003](http://dx.doi.org/10.1016/j.compositesb.2014.01.003).
16. D.J. Chang, Burst tests of filament-wound graphite–epoxy tubes, *J. Compos. Mater.* 37 (2003) 811–829, <http://dx.doi.org/10.1177/002199803031032>
17. ASTM D5685-11, Standard Specification for Fiberglass (Glass-Fiber-Reinforced Thermosetting-Resin) Pressure Pipe Fittings, ASTM International, West Conshohocken, PA, 2011, www.astm.org.
18. J.B. Romans, A.G. Sands, J.E. Cowling, Fatigue Behavior of Glass Filament-Wound Epoxy Composites in Water, *Industrial and Engineering chemistry product research and Development*, 11: 3, (1972) 261-268, [10.1021/i360043a004](http://dx.doi.org/10.1021/i360043a004)
19. J.V. Gauchel, I. Steg, J.E. Cowling, "Reducing the Effect of Water on the Fatigue properties of S-Glass Epoxy Composites," *Fatigue of Composite Materials*, ASTM STP 569, American Society of Testing and Material, 1975, pp.45-52.
20. ASTM, D570: Standard Test Method for water absorption of Plastics, ASTM International, 2010. [10.1520/D0570-98R10E01](http://dx.doi.org/10.1520/D0570-98R10E01).
21. ASTM, D2444: Standard Test Method for Determination of the Impact Resistance of Thermoplastic Pipe and Fittings by Means of a tup (Falling Weight), ASTM International, 2010, <http://dx.doi.org/10.1520/D2444-99R10.2>.
22. ASTM D1599-18, Standard Test Method for Resistance to Short-Time Hydraulic Pressure of Plastic Pipe, Tubing, and Fittings, ASTM International, West Conshohocken, PA, 2018, www.astm.org
23. ASTM D2992-18, Standard Practice for Obtaining Hydrostatic or Pressure Design Basis for "Fiberglass" (Glass-Fiber-Reinforced Thermosetting-Resin) Pipe and Fittings, ASTM International, West Conshohocken, PA, 2018, www.astm.org.
24. K. Imielińska, L. Guillaumat, The effect of water immersion ageing on low-velocity impact behaviour of woven aramid–glass fibre/epoxy composites, *Compos. Sci. Technol.* 64 (2004) 2271–2278, <http://dx.doi.org/10.1016/j.compscitech.2004.03.002>.

(2019) ; <http://www.jmaterenvironsci.com>